Ab Initio Study of RDX Decomposition Mechanisms

Christine J. Wu* and Laurence E. Fried

Lawrence Livermore National Laboratory, University of California, Livermore, California 94551

Received: February 25, 1997; In Final Form: June 17, 1997[⊗]

The mechanism of the gas phase unimolecular decomposition of hexahydro-1,3,5,-trinitro-1,3,5,-triazine (RDX) has been investigated using first principles gradient-corrected density functional theory. We have calculated the potential energy profile for two previously suggested dissociation channels: (I) $N-NO_2$ bond rupture, and (II) concerted ring fission to three methylenenitramine molecules. The activation barriers for channels I and II are predicted to be 34.2 and 52.5 kcal/mol at the B-PW91/cc-pVDZ level, respectively. We have performed a simple transition state theory analysis which indicates that the prefactors for channel I and II are roughly 7×10^{17} and 1×10^{17} s^{-1}, respectively. Thus, our results suggest that path I is the dominant channel in gas phase thermal RDX decomposition.

I. Introduction

Over the past two decades, much progress has been made in understanding the chemical and physical properties of high explosives, particularly in predicting denotion products.[1−3] Nevertheless, little is known regarding initiation processes due to the rapid and complex nature of initiation kinetics. It is generally believed that the initiation of energetic compounds starts from molecular decomposition followed by a series of exothermic chemical reactions. Thus, the kinetics of thermal decomposition is expected to provide some insight into energetic material initiation and stability. As a widely used high explosive and monopropellant, hexahydro-1,3,5,-trinitro-1,3,5,-triazine (RDX) is one of the most thoroughly studied energetic compounds. However, even simple questions such as the nature of the initial step in the thermal decomposition of RDX are still a subject of debate.

There are many suggested initial unimolecular steps in the thermal decomposition of RDX including $N-NO_2$ bond rupture, concerted ring fission to three $CH_2N_2O_2$, C−N bond cleavage, C−H bond dissociation, and transfer of an oxygen from the NO_2 to an adjacent CH_2.[4] Among them, the most supported mechanism for condensed phase decomposition is $N-NO_2$ bond rupture, shown in Figure 1 as the path I. The most recent supporting evidence for this mechanism was given by the transient IR laser pyrolysis experiments of Wight and Botcher.[5−7] For a solid RDX thin film, they found that the initial decomposition products relate mostly to the $N-NO_2$ bond rupture.[5,6] Their experiments on samples with isotopically labeled nitrogen also showed that decomposition of RDX is mostly unimolecular and involves the removal of only one NO_2.[7]

Concerted symmetric ring fission to three $CH_2N_2O_2$ molecules is another competing mechanism which has convincing experimental evidence.[8] This mechanism is shown in Figure 1 as the path II. Using infrared multiphoton dissociation (IRMPD) of RDX in a molecular beam, Zhao, Hintsa, and Lee[8] suggested that the RDX molecule dissociates via both paths I and II. They found that a branching ratio of 2:1 for path II over path I best matched their time of flight spectra. They concluded that the dominant channel is the symmetric ring fission (II), not the $N-NO_2$ bond cleavage (I). However, no conclusive evidence for the ring-fission has been reported in studies of liquid and solid RDX.

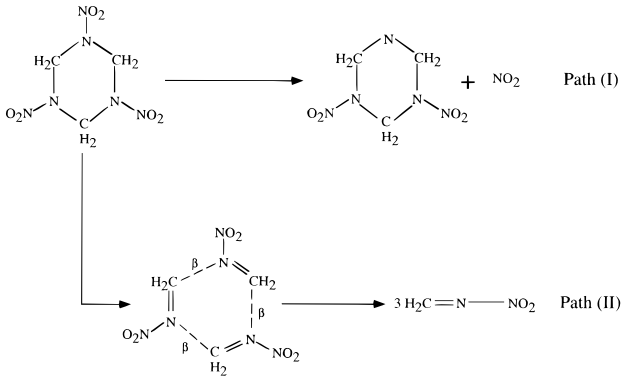

Figure 1. Schematic drawing of RDX dissociation via $N-NO_2$ bond rupture (path I) and symmetric ring-fission (path II).

The disagreement on the mechanism may be attributed to differing experimental conditions, such as phase of RDX, particle size, heating mechanism, heating rate, and pressure. It has been postulated that the solid and liquid confining environment may prohibit the ring fission reaction from proceeding.[5,7] The sample and experimental conditions were also suggested to qualitatively influence the measured global Arrhenius parameters for RDX thermal decomposition.[9] For instance, reported activation energies vary from 24.7 to 52.1 kcal/mol and reported preexponential factors vary from 10^{17} to 10^{20} s^{-1} for overall decomposition. Moreover, it is difficult to interpret the condensed phase experiments due to the many possible product species.

Gas phase molecular theory can be usefully compared to collision-free molecular beam experiments. Several theoretical studies related to gas phase RDX decomposition have been reported. Melius and Binkley[10] have estimated that the $N-NO_2$ bond dissociation energy is ∼48 kcal/mol, by comparison with smaller prototype molecular species. Their results rely on the assumption that RDX has a $N-NO_2$ bond dissociation energy similar to that of nitramine and methylnitramine. The barrier for the ring fission was calculated by Habibollahzadeh et al.[11] using the local density functional procedure with a Hartree−Fock (HF) optimized (STO-3G basis set) geometry. They reported a value of 72.2 kcal/mol, which is more than 20 kcal/mol higher than the reported global activation energy of RDX. Therefore, they did not consider ring fission to be the dominant mechanism of thermal gas phase decomposition.

[⊗] Abstract published in *Advance ACS Abstracts,* November 1, 1997.

S1089-5639(97)00678-6 CCC: $14.00

TABLE 1: Calculated RDX N−NO_2 Bond Dissociation Energy (D) and Heat of Reaction (ΔE) for RDX Ring Fission Dissociation Pathway[a]

	total energy (hartrees)					
	RDX	$H_6C_3N_5O_4$	NO_2	H_2CNNO_2	D_e (D_0) (kcal/mol)	ΔE_e (ΔE_0) (kcal/mol)
B-PW91/D95V	−897.283 61	−692.163 59	−205.053 78	−299.060 69	41.6 (37.1)	63.7 (54.5)
B-PW91/D95V+	−897.316 25	−692.187 35	−205.063 26	−299.073 82	41.2 (36.7)	59.5 (50.3)
B-PW91/D95V(d)	−897.580 22	−692.392 86	−205.127 64	−299.130 35	37.5 (33.0)	52.8 (43.6)
B-PW91/cc-pVDZ	−897.475 26	−692.312 67	−205.100 87	−299.166 34	38.7 (34.2)	51.0 (41.8)
B-LYP/D95V	−897.181 06	−692.067 42	−205.046 55	−299.033 11	42.1 (37.6)	51.3 (42.1)
B-LYP/D95+	−897.218 63	−692.095 07	−205.057 89	−299.046 87	41.2 (36.7)	48.9 (39.7)
B-LYP/cc-pVDZ	−897.351 19	−692.199 67	−205.088 57	−299.092 89	39.5 (35.0)	45.5 (36.3)
B3-PW91/D95V	−896.920 63	−691.894 39	−204.956 72	−298.932 21	43.6 (39.1)	77.8 (68.6)
B3-PW91/D95V+	−896.953 14	−691.916 83	−204.965 75	−298.944 60	44.3 (39.8)	74.9 (65.7)
B3-PW91/cc-pVDZ	−897.160 24	−692.075 45	−205.015 78	−299.018 34	43.3 (38.8)	66.0 (56.8)
B3-LYP/D95V	−897.262 96	−692.157 51	−205.037 81	−299.050 92	42.4 (37.9)	69.1 (59.9)
B3-LYP/D95V+	−897.296 87	−692.182 21	−205.047 89	−299.064 81	41.9 (37.4)	64.3 (55.1)
B3-LYP/cc-pvdz	−897.484 49	−692.324 00	−205.092 70	−299.130 54	42.5 (38.0)	58.3 (49.1)

[a] For D and ΔE, subscripts 0 and e refer to values before and after zero-point energy corrections, respectively.

The local density approximation (LDA)[12] employed by Habibollahzadeh et al.[11] has recently been shown to be unreliable for predicting barrier heights.[13−16] For example, for the $CH_3 + CH_4 \rightarrow CH_4 + CH_3$ reaction, LDA not only has an 86% error in the activation barrier but also gives a qualitatively incorrect double-well reaction profile.[14] A barrier height of 37 kcal/mol for ring fission was also suggested by Sewell and Thompson,[17] who used an indirect method to construct the potential energy surface of RDX. Chambers and Thompson[18] showed that the branching ratio of Zhao, Hintsa, and Lee[8] implies that the barrier must be less than 72 kcal/mol. Clearly, a reliable theoretical evaluation of RDX decomposition energetics for both pathways is critically needed.

The deficiencies of LDA in predicting molecular thermochemistry have been significantly overcome by recently developed gradient-corrected functionals in generalized gradient approximations (GGA). The promising performance of the GGA methods has been demostrated by a growing body of comparison studies.[13−16,19−35] For bond dissociation energies, gradient-corrected functionals such as Becke−Lee−Yang−Parr (B-LYP)[36,37] have been shown to be accurate to within a few kcal/mol.[13,21,23] Furthermore, it has been found that these methods can properly describe the complete dissociation curve using spin unrestricted formulations.[15,21] For transition state barrier heights, the performance of GGA methods are somewhat system dependent and still a subject of active research.[14−16,29−35] Roughly speaking, GGA gives much better results than LDA, and in many cases it provides a level of accuracy similar to other sophisticated ab initio methods.[14,15,29−31] It has been reported that GGA severely underestimates barrier heights for some reactions due to Coulomb "self-interaction" of the electrons.[16,30,31,35] However, this problem can be improved by mixing in part of the exact HF exchange.[16,31] The computational time of DFT methods formally scales as the number of electrons N^3. This compares favorably with other high-level quantum methods of similar accuracy, which scale as N^5 or greater. This makes DFT methods suitable for the study of large systems such as RDX. It is particularly encouraging that gradient-corrected DFT methods produce satisfactory results for nitrogen−oxygen chemical systems where traditional ab initio methods, such as MP2, have difficulties in giving geometries reasonably close to experimental values.[27]

In this paper, we present a detailed study of RDX unimolecular dissociation via path I and II using several recent gradient-corrected DFT methods. Our results provide a direct comparison to the gas phase RDX experiment[8] and thus help to clarify this controversial issue.

TABLE 2: Zero-Point Energy Corrections (kcal/mol) Obtained Using B-PW91 Functionals and D95V Basis Set[a]

RDX	$H_6C_3N_5O_4$	NO_2	TS	H_2CNNO_2
83.9	74.7	4.7	78.3	24.9

[a] TS refers to transition state of ring fission pathway.

II. Computational Details

All total energy calculations were performed using the Gaussian 94/DFT[38] package with spin-polarized gradient-corrected exchange and correlation functionals. The procedures are based on the spin-unrestricted Kohn−Sham[12] formalism. We have chosen four widely adopted and promising functionals: B-PW91, B3-PW91, B-LYP, and B3-LYP. B refers to the Becke's 1988 gradient-corrected exchange functional[36] which reproduces the exact asymptotic behavior of exchange energy density in finite system, and B3 refers to Becke's hybrid method of mixing Hartree−Fock exchange energy into the exchange functional.[39] PW91 and LYP are the gradient-corrected correlation functionals of Perdew-Wang,[40] and Lee, Yang, and Parr.[37] Three Gaussian-type basis sets were used for the Kohn−Sham orbital expansion: Dunning's valence double zeta (D95V),[41] D95V plus diffuse function (D95V+), and Dunning's most recent correlation consistent polarized valence double zeta basis sets (cc-pVDZ).[42] In order to examine the effect of the correlation-optimized cc-pVDZ basis set on DFT calculations, we compared the results obtained from the D95V(d)(D95V plus polarization functions) basis set with that from cc-pVDZ. Both basis sets have the same structure and size, except that cc-pVDZ is optimized with correlated atomic calculations.[42]

III. Results and Discussion

A. N−NO_2 Bond Cleavage. The results for the N−NO_2 bond dissociation energy (D) are presented in Table 1. D_e and D_0 refer to the values without and with zero-point correction of the vibrational energy (listed in Table 2), respectively, which was calculated at the B-PW91/D95V level. It is satisfying to see that the four functionals we used give consistent results. Although adding polarization functions has a larger effect than adding diffuse functions, neither changes the value of D significantly. For instance, the largest deviation between D95V and D95V+ is −0.9 kcal/mol (B-LYP), while that between D95V and cc-pVDZ is −2.9 kcal/mol (B-PW91). The effect of the correlation consistent basis set on DFT energies does not appear to be significant, since D95V(d) and cc-pVDZ have very similar results for the bond dissociation energy. The

TABLE 3: DFT/cc-pVDZ Results of N−NO_2 Bond Dissociation Energies (kcal/mol) for CH_3HNNO_2 and H_2NNO_2[a]

	B-PW91	B-LYP	B3-PW91	B3-LYP	other theories
H_2NNO_2	55.4(47.6)	52.8(45.0)	56.4(48.6)	54.5(46.7)	51.0(43.6),[b] 61.0(53.6)[c]
CH_3HNNO_2	51.5(44.3)	49.0(41.8)	53.5(46.3)	51.4(44.2)	(48.6)[d]

[a] Values without and with parentheses correspond to those without and with zero-point corrections, respectively. [b] From ref 43, using a configuration interaction (QCISD) method. [c] From ref 43, using Gaussian-2(G2) method. [d] From ref 10, using bond-additivity-corrected Møller−Plesset fourth-order perturbation (BAC-MP4) method.

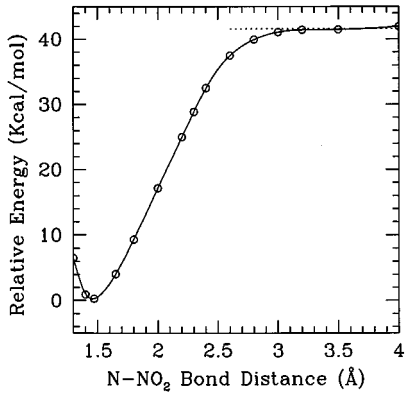

Figure 2. Potential energy curve for RDX dissociation via N−NO_2 bond rupture along the reaction coordinate (N−NO_2 bond). Circles represent the results of B-PW91/D95V and connected by the solid line. Energies are referenced to the RDX equilibrium. The dashed line indicates the dissociation limit.

deviation between the basis sets considered is roughly the same as the deviation between the functionals. Becke's hybrid B3 method gives a slightly higher value of the bond energy (∼4 kcal/mol) than Becke 88. Using our largest basis set (cc-pVDZ), four functionals give D_e ranging from 38.7 to 43.3 kcal/mol, with an average value of 41.0 kcal/mol and a maximum deviation of ±2.3 kcal/mol. Taking the zero-point energy correction into account, we predict that the N−NO_2 bond energy D_0 is 34.2 kcal/mol at the B-PW91/cc-pVDZ level.

Our DFT values for the N−NO_2 bond energy in RDX are significantly smaller than the previous estimate of ∼48 kcal/mol. The previous value was based on the assumption that the N−NO_2 bond in RDX is similar to that of methylnitramine and nitramine.[10] In order to figure out whether the disagreement is caused by different computational methods or by the assumed similarity to nitramine, we have performed calculations for nitramine (H_2NNO_2) and methylnitramine (CH_3NHNO_2) using selected gradient-corrected functionals and the cc-pVDZ basis set. The zero-point vibrational energy correction is obtained at the B-PW91/D95V level. Table 2 shows our N−NO_2 bond energies for nitramine and methylnitramine; they are consistent with previous theoretical predictions.[10,43] We conclude that RDX has a weaker N−NO_2 bond than nitramine and methylnitramine. Differences between computational methods play a secondary role in evaluating the previous estimate of the N−NO_2 bond energy.

There are two possible reasons for the smaller N−NO_2 bond dissociation energy for RDX; either geometric or electronic relaxations can occur through the RDX ring fragment ($H_6C_3N_5O_4$). To estimate the contribution of geometric relaxation, we calculated the energy difference between the rigid $H_6C_3N_5O_4$ and the relaxed $H_6C_3H_5O_4$. The rigid $H_6C_3N_6O_4$ is taken from the minimum geometry of RDX without a NO_2 group. As shown in Table 3, the RDX geometric stabilization is between 2 and 6 kcal/mol. Electronic relaxation is thus the dominant mechanism; it accounts for 6−10 kcal/mol.

We have mapped the potential energy curve (Figure 2) along the reaction coordinate to calculate the N−NO_2 bond dissociation barrier. The B-PW91 functional and D95V basis set were used. Our choice of the B exchange functional over B3 comes from consideration of spin contamination. Baker, Scheiner, and Andzelm[44] have found that spin contamination derives primarily from the exchange term, and unrestricted Kohn−Sham wave functions display much less spin contamination than their unrestricted HF counterparts. Therefore, the mixing of HF exchange energy in the B3 method is likely to introduce more spin contamination than B. Our choice of PW91 over LYP is mainly based on Perdew and Burke's[45] comparison, in which they suggested that PW91 is the best correlation functional. In comparison to PW91, the LYP functional does not satisfy several known exact formal conditions, such as the uniform electron gas limit. However, we realize that current understanding of the performance of GGA functionals in various contexts is still limited.

TABLE 4: Calculated RDX Geometric Relaxation Energy ($E_{relaxed}$, kcal/mol) Using cc-pVDZ Basis Set

	B-PW91	B-LYP	B3-PW91	B3-LYP
E_{relax}	5.8	2.5	2.9	1.6

Caution must be used in interpreting the significance of the deviation of the energy between functionals, since there is no known systematic procedure to improve the accuracy of exchange-correlation functionals. The success of exchange-correlation functionals depends partially on error cancellation between exchange and correlation parts. Therefore, it is not surprising to see that reported discrepancies between functionals range from negligible to sizable depending on the system of investigation.[35] For instance, Durant[35] has very recently reported average errors of −4.7 kcal/mol for B3-LYP and −5.4 kcal/mol for B3-PW91 when calculating a variety of small molecule transition state energies.

The potential energy profile displayed in Figure 2 was obtained by optimizing the geometry at each fixed, N−NO_2 separation (R(N−N)). We found that spin contamination appears at a N−NO_2 separation of 2.4 Å, about 1.6 times the N−NO_2 equilibrium bond distance, which is similar to a previous finding.[44] Our potential energy profile has zero barrier (the typical case for a radical recombination reaction). This is in agreement with the experimental observation that the product translational energy distribution for N−NO_2 bond rupture is peaked at zero.[8] Therefore, the barrier for breaking the N−N bond is approximately equal to N−NO_2 bond energy D_0.

B. Concerted Symmetric Ring Fission. The heat of reaction (ΔE) for the concerted symmetric ring fission (II) is listed in Table 1. It was calculated in the same fashion as the N−NO_2 bond dissociation energy. Note that the deviation between various exchange-correlation functionals and basis sets is larger than for pathway I. This may be due to the large change in the electronic character from RDX to H_2CNNO_2. However, this pathway involves rearrangement of three chemical bonds. If one estimates the deviation between functionals and basis sets based on the number of changing bonds, they are not too far from those of pathway I. For instance, Becke's hybrid method (B3) again gives consistently higher value (∼5 kcal/

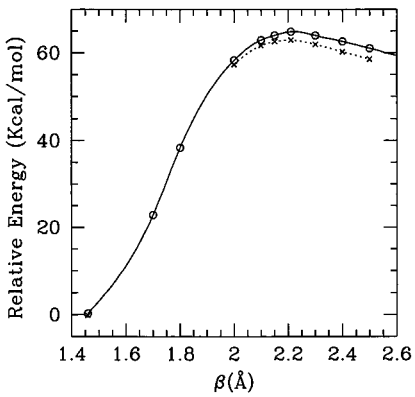

Figure 3. Potential energy curve for RDX ring fission along the reaction coordinate (the broken C−N bond, β). Circles and crosses represent the results of B-PW91/D95V and B-PW91/D95+ and are connected by solid and dashed lines, respectively. Energies are referenced to the RDX equilibrium.

mol per bond) than Becke 88. Nevertheless, the heat of reaction for the ring fission is systematically higher than the N−NO_2 bond dissociation energy within the same functional and basis set. Using the largest basis set cc-pVDZ, four functionals give ΔE ranging from 66.0 to 45.5 kcal/mol, with an average value of 55.2 and maximum deviation of ±10.2 kcal/mol. Taking the zero-point energy correction of 9.2 kcal/mol, our best estimate at the B-PW91/cc-pVDZ level for the heat of reaction of the concerted ring fission is 41.8 kcal/mol.

We have mapped the potential energy profile of the ring fission (see Figure 3) in order to identify the transition state. The reaction coordinate parameter β was chosen to be the three alternate C−N distances along the breaking C−N bonds (indicated as the dashed line in Figure 1). At each β, we optimized all other degrees of freedom at both B-PW91/D95V and B-PW91/D95V+ level. Although adding diffuse functions lowers the potential energy, the energy profiles of the D95V and D95V+ basis sets have a similar shape, including the same β of 2.21 Å at the saddle point. We have assumed that cc-pVDZ has the same β value for the saddle point; therefore, the transition state at the cc-pVDZ level was obtained by optimizing all other degree of freedoms while keeping β at 2.21 Å. This B-PW91/cc-pVDZ calculation gives a transition state height of 58.1 kcal/mol. This transition state was found to be spin-pure, indicating DFT's ability to maintain pure spin for the transition state within a single determinant. In addition, the spin-pure character remains all the way up to the largest β value (2.5 Å) that we have calculated. The Hessian calculation at the B-PW91/D95V level shows one imaginary frequency for the predicted transition state. Taking into account the zero-point energy correction, our best estimate of barrier height at B-PW91/cc-pVDZ level for pathway II is 52.5 kcal/mol. Note that this value is about 20 kcal/mol smaller than the previous LDA result.[11]

The geometries of RDX obtained from various functionals using cc-pVDZ basis set are listed in Table 5. The deviations between functionals are similar to those between experiments.[46,47] In general, DFT results are in good agreement with the experimental[46,47] values and the previous HF result.[11] Table 6 tabulates the geometry of the transition state obtained at B-PW91/cc-pVDZ level (except for β which is obtained at B-PW91/D95+). Note that the shorter C−N bond in the transition state (indicated as the "double" bond in Figure 1) is 1.306 Å, which is slightly longer than the true C−N double bond of 1.281 Å of the final dissociation product, $CH_2N_2O_2$, but significantly shorter than the C−N bond length of 1.454 Å in RDX. Our β of 2.21 Å is slightly larger than the previous HF result of 2.07.[11] Overall, there is a similar level of agreement between HF and DFT geometries for the equilibrium and transition state.[11]

A detailed comparison between path I and path II requires the evaluation of not only the barriers but also the reaction prefactors. Rough estimates can be made from simple kinetic and transition state theory. For the path I reaction, the rate constant $k^{(I)}$ of N−NO_2 dissociation was computed as $k_b^{(I)}K_{equil}^{(I)}$, where $k_b^{(I)}$ is the rate constant for the backward radical recombination reaction and $K_{equil}^{(I)}$ is the equilibrium constant of reaction I, respectively. For the path II reaction, the rate constant $k^{(II)}$ was calculated using transition state theory.[51] We evaluated $k_b^{(I)}$ using the Gorin model[48−50] in which the reaction is assumed to proceed when the attractive force is larger than the centrifugal force. The parameters in the Gorin model are the reduced masses of fragments and the attractive force constant in the assumed inverse R^6 potential. We estimated the attractive force constant from the tail of our DFT potential. This model has been applied to polyatomic molecules with reasonable results.[49,50] As an example, $k_b^{(I)}$ is calculated to be 2.8×10^{13} cm^3/(mol s) at a temperature of 400 K, which is a typical rate for radical recombination. In calculations of $K_{equil}^{(I)}$ and $k^{(II)}$, we applied the harmonic approximation in evaluating the vibrational partition functions and included both rotational and electronic contributions. Given the B-PW91/cc-pVDZ activation barriers, Arrhenius parameters for paths I and II are estimated to be $E_a^{(I)} = 34.3$ kcal/mol, $A^{(I)} = 7.3 \times 10^{17}$ s^{-1}, and $E_a^{(II)} = 54.7$ kcal/mol, $A^{(II)} = 1.3 \times 10^{17}$ s^{-1}, respectively. The Arrhenius barrier E_a for both (I) and (II) are very similar to the zero temperature results. Since the prefactors for path I and II are of the same order of magnitude, we predict path I to be the dominant channel due to its lower activation barrier.

It should be emphasized that the methods used to find the prefactor are more qualitative (order of magnitude accuracy) than quantitative. It is somewhat surprising that the simple homolysis of one bond has a prefactor similar to that of a reaction involving three bond fissions. This may be due to other geometric factors. For instance, path I produces one floppy molecule, while the three fragments from path II are more

TABLE 5: Calculated RDX Geometries Using cc-pVDZ Basis Set[a]

parameters	B-PW91	B-LYP	B3-PW91	B3-LYP	HF[11]	exp[46,47]
C−N	1.454	1.470	1.450	1.459	1.49	1.44−1.47, 1.464
C−H	1.106, 1.111	1.102, 1.109	1.092, 1.102	1.091, 1.101	1.09	1.06−1.09, 1.089
N−N	1.422	1.469	1.394	1.421	1.48	1.35−1.40, 1.413
N−O	1.232	1.235	1.214	1.218	1.27	1.20−1.23, 1.213
CNC	119.8	117.3	116.7	116.0	115	114.6−115.1, 123.7
NCN	110.8	113.4	119.6	112.6	115	107.8−111.7, 109.4
HCN	107.8, 110.2	108.7, 107.9	109.6, 108.2	109.4, 107.6	107−108	106.9−111.3
NNC	118.9	117.1	119.6	117.7	113	115.6−120.9, 116.3
ONN	115.7	116.1	116.5	116.4	117	116.8−117.8, 117.2
NNCN	239.4	254.5	249.8	258.7		

[a] Bond lengths and bond angles are in units of Å and deg, respectively.

TABLE 6: Calculated Transition State Geometry for Ring Fission[a]

parameters	B-PW91/cc-pVDZ	HF[11]
C−N	1.306, 2.210	1.32, 2.07
C−H	1.101, 1.098	1.09
N−N	1.499	1.50
N−O	1.226	1.27
CNC	118.6	120
NCN	113.2	108
HCN	121.4, 116.6	117−121
NNC	113.2	115
ONN	116.6	115−119
NNCN	274.3	

[a] Bond lengths and bond angles are in units of Å and deg, respectively.

stiff. Therefore, the relative entropy change of path I and II may be less than expected based on the number of fragments alone.

IV. Summary

We have investigated the mechanism of the gas phase unimolecular decomposition of RDX. Among all possible reaction pathways, we considered only two specific reaction channels. $N-NO_2$ bond rupture and symmetric concerted ring fission, since they are best supported by experiments. A range of basis sets and modern gradient-corrected density functional methods were applied to this problem, in order to ensure that the final conclusion does not depend on computational methods. We have found that the activation barrier for concerted ring fission is roughly 18 kcal/mol greater than that for $N-NO_2$ bond rupture, a difference that is significantly larger than the maximum deviation found between different functionals. This suggests that thermal gas phase decomposition at temperatures significantly under 18 kcal/mol (∼9000 K) most likely proceeds via $N-NO_2$ bond rupture. In addition, simple kinetic and transition state theory calculations indicate that the prefactors for these two paths differ very little, and thus they do not play a significant role in differentiating the rates. Although more sophisticated kinetic rate theories such as variational transition state theory and anharmonicity may change the prefactor by a factor of 6 or greater,[52] the uncertainties in our estimated prefactors are small compared to the difference in barrier heights at temperatures of interest. In the future our results could be used in constructing improved classical potentials for RDX; this would then allow a more detailed comparison of the branching ratios of the two mechanisms as a function of temperature and excitation mechanism.

Acknowledgment. This work was performed under the auspices of the U.S. Department of Energy by the Lawrence Livermore National Laboratory under contract No. W-7405-ENG-48.

References and Notes

(1) Fickett, W.; Davis, W. C. *Detonation*; University of California Press: Los Angeles, 1979.
(2) Ree, F. H. *J. Chem. Phys.* **1984**, *81*, 1251.
(3) Fried, Laurence E.; Souers, P. Clark *Propellants, Explos. Pyrotech.* **1996**, *21*, 215.
(4) Behrens, R. *Chemistry and Physics of Energetic Materials*; Bulusu, S. N., Ed.; Kluwer: Dordrecht, The Netherlands, 1990; p 347.
(5) Wight, C. A.; Botcher, T. R. *J. Am. Chem. Soc.* **1992**, *114*, 8303.
(6) Botcher, T. R.; Wight, C. A. *J. Phys. Chem.* **1993**, *97*, 9149.
(7) Botcher, T. R.; Wight, C. A. *J. Phys. Chem.* **1994**, *98*, 5541.
(8) Zhao, X. S.; Hintsa, E. J.; Lee, Y. T. *J. Chem. Phys.* **1988**, *88*, 801.
(9) Brill, T. B.; Gongwer, P. E.; Williams, G. K. *J. Phys. Chem.* **1994**, *98*, 12242.
(10) Melius, C. F.; Binkley, J. S. *Twenty-first Symposium (International) on Combustion, [Proceedings]*; The Combustion Institute, 1986, p 1953.
(11) Habibollahzadeh, D.; Grodzicki, M.; Seminario, J. M.; Politzer, P. *J. Phys. Chem.* **1991**, *95*, 7699.
(12) Kohn, W.; Sham, L. *Phys. Rev. A* **1965**, *140*, 1133.
(13) Kohn, W.; Becke, A. D.; Parr, R. G. *J. Phys. Chem.* **1996**, *100*, 12974.
(14) Fan, L.; Ziegler, T. *J. Am. Chem. Soc.* **1992**, *114*, 10890.
(15) Andzelm, J.; Sosa, C.; Eades, R. A. *J. Phys. Chem.* **1993**, *97*, 4664.
(16) Johnson, B. G.; Gonzales, C. A.; Gill, P. M. W.; Pople, J. A. *Chem. Phys. Lett.* **1994**, *221*, 100.
(17) Sewell, T. D.; Thompson, D. L. *J. Phys. Chem.* **1991**, *95*, 6229.
(18) Chambers, C. C.; Thompson, D. L. *J. Phys. Chem.* **1995**, *99*, 15881.
(19) Fitzgerald, G.; Andzelm, J. *J. Phys. Chem.* **1991**, *95*, 10531.
(20) Andzelm, J.; Wimmer, E. *Physica B* **1991**, *172*, 307.
(21) Andzelm, J.; Wimmer, E. *J. Chem. Phys.* **1992**, *96*, 1280.
(22) Gill, P. M. W.; Johnson, B. G.; Pople, J. A. *Chem. Phys. Lett.* **1992**, *197*, 499.
(23) Johnson, B. G.; Gill, P. M. W.; Pople, J. A. *J. Chem. Phys.* **1993**, *98*, 5612.
(24) Seminario, J. M. *Int. J. Quantum Chem.* **1994**, *28*, 655.
(25) Chermette, H.; Lembarki, A.; Gulbinat. P.; Weber, J. *Int. J. Quantum Chem.* **1995**, *56*, 753.
(26) Holthausen, M. C.; Heinemann, C.; Cornehl, H. H.; Koch, W.; Schwarz, H. *J. Chem. Phys.* **1995**, *102*, 4931.
(27) Jursic, B. S. *Int. J. Quant. Chem.* **1996**, *58*, 41.
(28) Barone, V.; Adamo, C.; Mele, F. *Chem. Phys. Lett.* **1996**, *249*, 290.
(29) Scuseria, G. E. *J. Chem. Phys.* **1992**, *97*, 7528.
(30) Andzelm, J.; Baker, J.; Scheiner, A.; Wrinn, M. *Int. J. Quantum Chem.* **1995**, *56*, 733.
(31) Baker, J.; Andzelm, J.; Muir, M. *J. Chem. Phys.* **1995**, *102*, 2063.
(32) Baker, J.; Andzelm, J.; Muir, M.; Taylor, P. R. *Chem. Phys. Lett.* **1995**, *237*, 53.
(33) Truong, T. N.; Duncan, W. *J. Chem. Phys.* **1994**, *101*, 7408.
(34) Zhang, Q.; Bell, R.; Truong, T. N. *J. Phys. Chem.* **1995**, *99*, 592.
(35) Durant, J. L. *Chem. Phys. Lett.* **1996**, *256*, 595.
(36) Becke, A. D. *Phys. Rev. A* **1988**, *38*, 3098.
(37) Lee, C.; Yang, W.; Parr, R. G. *Phys. Rev. B* **1988**, *37*, 785.
(38) Frisch, M. J.; Trucks, G. W.; Schlegel, H. B.; Gill, P. M. W.; Johnson, B. G.; Robb, M. A.; Cheeseman, J. R.; Keith, T. A.; Petersson, G. A.; Montgomery, J. A.; Raghavachari, K.; Al-Laham, M. A.; Zakrzewski, V. G.; Ortiz, J. V.; Foresman, J. B.; Cioslowski, J.; Stefanov, B. B.; Nanayakkara, A.; Challacombe, M.; Peng, C. Y.; Ayala, P. Y.; Chen, W.; Wong, M. W.; Andres, J. L.; Replogle, E. S.; Gomperts, R.; Martin, R. L.; Fox, D. J.; Binkley, J. S.; Defrees, D. J.; Baker, J.; Stewart, J. P.; Head-Gordon, M.; Gonzalez, C.; Pople, J. A. *Gaussian 94*; Gaussian, Inc.: Pittsburgh, PA, 1995.
(39) Becke, A. D. *J. Chem. Phys.* **1993**, *98*, 5648.
(40) Perdew, J. P.; Wang, Y. *Phys. Rev. B* **1992**, *45*, 13244.
(41) Dunning, T. H., Jr.; Hay, P. J. *Modern Theoretical Chemistry*; Plenum: New York, 1976.
(42) Dunning, T. H., Jr. *J. Chem. Phys.* **1989**, *90*, 1007.
(43) Seminario, J. M.; Politzer, P. *Int. J. Quantum Chem., Quantum Chem. Symp.* **1992**, *26*, 497.
(44) Baker, J.; Scheiner, A.; Andzelm, J. *Chem. Phys. Lett.* **1993**, *216*, 380.
(45) Perdew, J. P.; Burke, K. *Int. J. Quant. Chem.* **1996**, *57*, 309.
(46) Choi, C. S.; Prince, E. *Acta Crystallogr.* **1972**, *B28*, 2857.
(47) Shishkov, I. F.; Vilkov, L. V.; Kolonits, M.; Rozsondai, B. *Struct. Chem.* **1991**, *2*, 57.
(48) Gorin, E. *Acta Physicochem. U.S.S.R* **1938**, *9*, 661.
(49) Johnson, H. S.; Goldfinger, P. *J. Chem. Phys.* **1962**, *37*, 700.
(50) Johnston, H. S. *Gas Phase Reaction Rate Theory*; Ronald: New York, 1966.
(51) Bennett, C. H. *Algorithms for Chemical Computations:* ACS Symposium Series, Vol. 46; Am. Chem. Soc.: Washington, DC, 1977.
(52) Truhlar, D. G.; Garrett, B. C.; Klippenstein, S. J. *J. Phys. Chem.* **1996**, *100*, 12771.